Title

A murine model of *Trypanosoma brucei*-induced myocarditis and cardiac dysfunction

Authors

Nathan Crilly[1,2], Marcelle Dina Zita[3], Alexander Beaver[1,2], Polina Sysa-Shah[1,4], Aashik Bhalodia[3], Kathy Gabrielson[1], Luigi Adamo[*3,] Monica R. Mugnier*[1,2]

*Co-Senior authors

Affiliations

[1] Department of Molecular and Comparative Pathobiology, School of Medicine, Johns Hopkins University, Baltimore, Maryland, USA

[2] Department of Molecular Microbiology and Immunology, Johns Hopkins Bloomberg School of Public Health, Baltimore, Maryland, USA

[3] Division of Cardiology, Department of Medicine, School of Medicine, Johns Hopkins University, Baltimore, Maryland, USA

[4] Molecular Imaging Service Center and Cancer Functional Imaging Core, School of Medicine, Johns Hopkins University, Baltimore, Maryland, USA

Abstract

Trypanosoma brucei is a protozoan parasite that causes human and animal African trypanosomiases (HAT and AAT). Cardiac symptoms are commonly reported in HAT patients, and intracardiac parasites with accompanying myocarditis have been observed in both natural hosts and animal models of *T. brucei* infection. However, despite the importance of *T. brucei* as a cause of cardiac dysfunction and the dramatic socioeconomic impact of African trypanosomiases in sub-Saharan Africa, there are currently no reproducible murine models of *T. brucei*-associated cardiomyopathy. We present the first clinically relevant, reproducible murine model of cardiac dysfunction in chronic *T. brucei* infection. Similar to humans, mice showed histological evidence of myocarditis and elevation of serum NT-proBNP. Serum NT-proBNP levels were elevated prior to the development of severe ventricular dysfunction. On flow cytometry, myocarditis was associated with an increase of most myocardial immune cell populations, including multiple T cell and macrophage subsets, corroborating the notion that *T. brucei*-associated cardiac damage is an immune-mediated event. This novel mouse model represents a powerful and practical tool to investigate the pathogenesis of *T. brucei*-mediated heart damage and support the development of therapeutic options for *T. brucei*-associated cardiac disease.

Introduction

The threat of *Trypanosoma brucei* is a fact of life throughout sub-Saharan Africa. A protozoan parasite spread by the tsetse fly vector, *T. brucei* is the causative agent of two neglected tropical diseases, human and animal African trypanosomiasis (HAT and AAT) [1]. In both humans and animals, the disease is characterized by waxing and waning fever followed by chronic wasting and a coma which gives the disease its historical name, "sleeping sickness" [2,3]. Although HAT is uncommon, with fewer than 1000 cases reported in 2019 through 2020, the ubiquity of animal reservoirs and the insect vector throughout sub-Saharan Africa means that re-emergence is a constant threat [4–7]. In addition to the direct impacts on human health, AAT is a severe burden to animal agriculture throughout sub-Saharan Africa and a serious contributor to food insecurity in the region, with an estimated cost of $4.75 billion per year and an incalculable impact on individual livelihoods [8].

T. brucei is often thought of as a parasite of the hemolymphatics and central nervous system. However, both historical and recent studies have led to a renewed appreciation for *T. brucei* as a parasite of extravascular spaces [9,10]. *T. brucei* parasites invade and colonize multiple extravascular tissues, including the heart, lungs, adipose tissue, skin, eyes, gonads, pancreas, and brain [11,12]. Within these spaces, tissue-resident parasites are associated with widespread inflammation and damage, resulting in loss of organ function that contributes to mortality [9,10,13].

T. brucei colonizes the heart, and cardiac disease is a likely contributor to HAT mortality [14,15]. HAT patients exhibit elevated cardiac NT-proBNP, a biomarker which is a sensitive predictor of heart failure and 19% report at least one symptom consistent with heart failure[15]. One study found that patients in Cameroon with dilated cardiomyopathy were significantly more likely to have anti-trypanosomal antibodies than healthy controls, suggesting that even clinically inapparent *T. brucei* infection might contribute to cardiac dysfunction[16]. In agreement with these clinical findings, myocarditis has been reported in autopsies of patients who have died from HAT, suggesting that cardiac inflammation is a contributor to *T. brucei*-associated cardiac disease [17,18].

Unfortunately, while there is clear evidence that cardiac disease is a consequence of African trypanosomiasis., *T. brucei*-associated heart disease remains understudied. In particular, there has been a lack of a well-established animal models to allow detailed investigation into the pathology, pathogenesis, and functional consequences of *T. brucei*-associated heart disease. Several historical studies have described the histopathology of myocarditis during *T. brucei* infection, especially in large animal models such as cattle, dogs, and nonhuman primates [19–22]. While large animal models, especially primates, accurately recapitulate human disease, the expense, difficulty, and ethical issues of working with such model species has prevented their widespread adoption by *T. brucei* researchers. More recently, researchers have published a rat model of acute cardiac disease during early *T. brucei* infection. In this acute model, infected rats exhibited myocarditis and ventricular arrhythmias at 11 days postinfection (dpi), similar to the pathological and EKG findings reported in human patients [15,18,23,24]. Although the rat model demonstrates that *T. brucei*-related cardiac disease can be recapitulated in a rodent, there are important limitations. Notably, studies in the rat have been limited to the first two weeks of infection, while clinical data suggest that cardiac symptoms and myocarditis are most prominent

during chronic HAT [17,18]. In addition, studies in the rat model have been limited to analyzing histopathology and EKG findings, although other modalities such as echocardiography and measurement of cardiac biomarkers are important for assessing the severity and progression of heart disease. Finally, there are relatively few tools for genetic and immunological manipulations in the rat, potentially limiting its usefulness for investigating disease pathogenesis [25] .

A mouse model of *T. brucei*-associated cardiac disease would have multiple advantages. Compared to other animal models, mice are relatively inexpensive, safe, and simple to handle and house, making them practical for most investigators. In addition, there are numerous well-characterized strains and knockout lines of mice, allowing detailed investigation into disease mechanisms [25]. Mice are also well-characterized as a model species for a variety of parasitic diseases, including those caused by African (*T. brucei*) and New World (*Trypanosoma cruzi*) trypanosomes [26,27]. Historical studies showed evidence of myocarditis in T. brucei-infected mice via histopathology, further supporting the utility of the mouse as a model of *T. brucei*-associated cardiac disease, although the consequences of this inflammation were not evaluated [28,29]. Overall, the establishment of a robust mouse model would allow for a detailed investigation into the mechanisms and consequences of *T. brucei*-associated cardiac disease and would be instrumental to the development of novel therapeutic options.

In this study, we present the first reproducible, clinically relevant, murine model of African Trypanosomiasis optimized to characterize the functional changes and immunology of *T. brucei*-associated cardiac disease.

Results

T. brucei infection induces elevation in NT-ProBNP prior to a reduction in left ventricular ejection fraction

Trypanosomiasis can be induced in mice by injecting viable *T. brucei* parasites into the tail vein of the mouse, resulting in a disease which is generally fatal within 30-40 days of infection [9,30]. To evaluate *T. brucei*-associated cardiac dysfunction, we infected adult male and female C57Bl/6J mice intravenously with 5-25 *T. brucei* parasites. At 28 days postinfection (dpi)—a commonly used timepoint to represent chronic *T. brucei* infection—we evaluated cardiac biomarkers and function [30].

We measured cardiac NT-proBNP as a biomarker of cardiac dysfunction. Cardiac NT-proBNP is a sensitive marker of heart failure [31]. Released from cardiomyocytes under conditions of excess stretch due to pressure or volume overload, [NO_PRINTED_FORM]NT-proBNP is elevated in HAT patients[15]. Plasma NT-proBNP concentrations were significantly increased in infected mice at 28 dpi (Figure 1A). NT-proBNP levels were slightly more elevated in male than in female mice, although this difference was not statistically significant (Supp. Fig. 2A).

We used echocardiography under sedation at 28 dpi to evaluate heart function. Infected mice had significantly increased ejection fraction and fractional shortening at 28 dpi (Fig 1B). Ejection

fraction was slightly higher in infected males than in females, although this difference was not statistically significant (Supp. Fig. 2B).

To further explore our observations, we repeated our functional assessments at 33 dpi, the latest timepoint at which mice can be experimentally manipulated before they begin to succumb to disease. Unsurprisingly, plasma NT-proBNP was again significantly elevated, with the mean NT-proBNP concentration (173.5 pg/mL) being similar to that observed at 28 dpi (165.4 pg/mL) (Fig. 1C). Interestingly, at 33 dpi mice exhibited a decreased ejection fraction, opposite to what was seen at 28 dpi (Fig. 1D). This could indicate cardiac decompensation as mice approach terminal status. It should be noted that, due to the fragility of mice at 33 dpi, echocardiography was performed awake, a technique that typically results in higher measured ejection fraction. Therefore, our findings indicate a significant drop in cardiac contractility between 28 dpi and 33 dpi.

T. brucei colonizes the myocardial interstitial space and causes myocarditis

Within the mammalian host, parasites live extracellularly and colonize multiple extravascular spaces, including the heart, ultimately causing fatal disease [1212,13]. To confirm the presence of intracardiac parasites in our model and to demonstrate that these parasites are extravascular, we infected adult C57Bl/6J mice with genetically modified *T. brucei* parasites that constitutively express the tdTomato fluorescent protein [3535]. This parasite line has previously been shown to exhibit similar infection dynamics as wild-type *T. brucei* parasites [12,35]. Mice were sacrificed at 14 dpi, a timepoint when extravascular parasite populations have been established and can be demonstrated on microscopy [9,12]. After sacrifice, we perfused mice to remove intravascular parasites, collected the heart, and performed immunofluorescence for CD31 to visualize the vasculature. *T. brucei* parasites were identified within the interstitial spaces of the heart. Intracardiac parasites localized separately from CD31-lined spaces, indicating that intracardiac parasites are extravascular (Fig 2).

To evaluate cardiac pathology due to *T. brucei* infection, we performed histopathology on the hearts of 6 *T. brucei*-infected mice at 28 dpi. Of the 6 hearts evaluated, 5 met the Dallas Criteria for lymphocytic myocarditis, while the sixth exhibited borderline myocarditis [36]. To further characterize histopathological changes, we used an established grading system to semi-quantitatively evaluate the severity of myocarditis (Table 1) [37]. At 28 dpi, all mice exhibited myocarditis, with an average histological grade of 2, indicating moderate multifocal myocarditis (Fig 3A). Inflammation affected all layers of the heart, including endocardium, myocardium, and epicardium, and the inflammation was primarily mononuclear, with large numbers of lymphocytes, plasma cells, and macrophages. Necrosis was not a major feature. The severity of inflammation was most severe in the atria and at the atrioventricular (AV) junction (Fig 3B). The pattern and severity of inflammation observed were consistent with previous histopathology findings in humans and natural hosts [18–22,28,38,39].

178 **Immune cell populations in the heart are consistent with immune-mediated myocarditis**
179
180 We had identified myocarditis as a consequence of *T. brucei* infection, and previous research has
181 indicated that the host immune response may contribute to *T. brucei*-associated cardiac
182 pathology [28]. To better understand the intracardiac immune response to *T. brucei*, we performed
183 flow cytometry at 28 dpi to characterize the immune cell population in the heart. Numbers of
184 CD45+ cells/mg of tissue were markedly elevated in the hearts of all infected mice at 28 dpi,
185 supporting our histopathological finding of myocarditis (Fig 4A).
186
187 Examining individual cell populations, most immune cell lineages were more abundant in *T.*
188 *brucei* infected hearts than in age-matched controls (Fig 4B-C). In agreement with the functional
189 data, most immune cell populations were slightly more elevated in males than in females,
190 although the difference was not statistically significant for any cell lineage (Supp. Fig 2E-F).
191
192 Numbers of both CD4+ T cells and macrophages were significantly increased in infected hearts,
193 which is unsurprising, since these cell types are necessary for an effective immune response to
194 African trypanosomes (Fig 4B-C) [40]. Of the different macrophage subsets, the CCR2^{hi}MHC-II^{hi}
195 population experienced the largest increase. This subset represents pro-inflammatory, monocyte-
196 derived macrophages, indicating that *T. brucei* infection causes an influx of pro-inflammatory
197 macrophages into the heart [41,42]. There was also a significant elevation of both CD8+ T cells and
198 natural killer (NK) cells, even though cell-mediated immunity is relatively ineffective at
199 responding to *T. brucei,* which is an extracellular parasite [43,4441,42].
200
201
202 **<u>Discussion</u>**
203
204 *T. brucei*-associated cardiac disease is an underappreciated and understudied aspect of African
205 trypanosomiasis. Here we report a reproducible murine model of *T. brucei* infection optimized to
206 investigate acute and chronic *T. brucei*-associated cardiac disease. We demonstrate that this
207 model recapitulates key aspects of *T. brucei*-associated cardiac disease in humans and natural
208 hosts, including the presence of intracardiac parasites, myocarditis, and elevated NT-proBNP.
209 Using this model, we learned that *T. brucei* infection results in parasite colonization of the
210 myocardial extracellular space and elevation of NT-proBNP (Figures 1-2). NT-proBNP elevation
211 was initially present in the context of a preserved ejection fraction, but the infection eventually
212 resulted in severe cardiac dysfunction (Figure 2). At a histological level, we found that
213 myocardial colonization by the parasite triggered a severe myocarditis characterized by
214 cardiomyocyte damage (Figure 3) and a multilineage inflammatory infiltrate (Figure 4). These
215 findings advance our understanding of the host-pathogen interactions in the heart, suggesting that
216 cardiac dysfunction associated with *T. brucei* infection is an immune-mediated event, potentially
217 providing valuable information to inform the development of novel targeted therapies for
218 animals and humans affected by African trypanosomiases.
219
220 Animal models have been used to study *T. brucei* infection since the early 1900s, and the first
221 attempts to use a murine model to investigate *T. brucei*-associated cardiac disease were
222 published in the late 1970s [14,28,29] . In these historical murine studies, investigators demonstrated

223 cardiac lesions in infected mice and showed that immunosuppression was associated with a
224 reduction in the size and frequency of inflammatory cardiac lesions [28]. However, despite their
225 seminal nature, these studies were limited in the scope of their investigation, primarily focusing
226 on histopathology and lacking more detailed functional or immunological assessments.
227 Moreover the studies were performed using infection protocols and parasite lines which were not
228 standardized, thus making their methods difficult to replicate. Our present work expands
229 significantly on those historical studies as it presents a reproducible method to generate cardiac
230 damage and dysfunction in a murine model, demonstrably recapitulating multiple aspects of
231 natural disease.
232
233 We have found that mice infected with *T. brucei* initially exhibit elevation in NT-proBNP in the
234 context of a preserved left ventricular ejection fraction. At 28 dpi, when we initially assessed
235 BNP, the mice had clear histological evidence of myocarditis. NT-proBNP is elevated in
236 response to an increase in intracardiac filling pressures [31]. In the context of a normal ejection
237 fraction and cardiac pathology BNP elevation is highly suggestive of Heart Failure with
238 Preserved Ejection fraction (HFpEF), a clinical condition characterized by reduced cardiac
239 performance and symptoms of heart failure despite a seemingly normal cardiac contractility[32].
240 However, BNP elevation in the context of a normal ejection fraction has also been described in
241 patients with acute myocarditis, likely as a result of stiffening of cardiac walls triggered by the
242 intracardiac immune response [33,34]. The potential overlap between myocarditis with preserved
243 ejection fraction and elevated BNP and HFpEF is an area that has not been properly investigated
244 so far in the clinical setting. However, taken together, our findings suggest that colonization of
245 the cardiac interstitium by *T. brucei* might result in a stiffening of cardiac walls and elevation of
246 cardiac pressures compatible with HFpEF, and that the myocarditic immune response triggered
247 by the parasites likely plays a key role in this process.
248
249 We used flow cytometry to investigate the intracardiac immune milieu during *T. brucei*
250 infection. Previous studies in humans and large animal models have found that the major
251 immune effectors during *T. brucei* infection are B cells, CD4+ T cells, and macrophages, which
252 are all necessary for a protective anti-trypanosomal immune response [40]. On the other hand,
253 CD8+ T cells and natural killer (NK) cells are thought to be mediators of pathological
254 inflammation in *T. brucei* infection, and their activation is associated with worse clinical
255 outcomes [40,43,44]. In agreement with our histopathological finding of myocarditis, we found that
256 most intracardiac immune cell populations were elevated, especially CD4+ and CD8+ T cells,
257 macrophages, and NK cells. The most highly elevated macrophage subset was the $CCR2^{hi}MHC$-
258 II^{hi} population, which represents pro-inflammatory, monocyte-derived macrophages [41,42]. Such
259 pro-inflammatory macrophages are necessary for an effective immune response to *T. brucei* [40].
260 However, switching to an anti-inflammatory macrophage phenotype is important for long-term
261 survival in experimentally infected animals, which suggests that an imbalance between pro-
262 inflammatory and anti-inflammatory macrophages could be a contributor to myocarditis in our
263 model [45]. The elevation of CD8+ T cells and NK cells in the heart are further suggestive of
264 immunopathology as a contributor to cardiac damage. Increases in these cell populations are
265 suggestive of a response to intracellular antigens, although *T. brucei* is entirely extracellular
266 throughout its life cycle [43]. Since CD8+ T cells are not a major feature of the immune response to

extracellular pathogens, we hypothesize that their elevation in our model indicates a response to cardiac self-antigens, indicating an auto-immune component of the observed myocarditis.

This hypothesis is corroborated by other evidence suggesting that *T. brucei*-associated organ damage has an auto-immune component. A recent study found that meningeal B cells produce high-affinity autoantibodies during *T. brucei* infection, suggesting that autoimmune responses may be a component of *T. brucei*-associated pathology in multiple tissues[46]. Clinically, cardiomyopathy patients in Cameroon have been found to have high levels of both anti-trypanosomal and anti-heart antibodies, further indicating a connection between *T. brucei* infection and autoimmune heart disease[16].

Furthermore, we hypothesize that immunopathology in the heart during *T. brucei* infection follows a similar process to the pathogenesis of Chagas cardiomyopathy, caused by the New World trypanosome *Trypanosoma cruzi.* The leading theory to explain the pathogenesis of Chagas disease posits that parasite colonization of the heart induces inflammation and release of self-antigens, resulting in a breakdown of self-tolerance and immune destruction of cardiomyocytes [47]. With chronicity, loss of cardiac muscle and replacement with scar tissue causes a collapse in cardiac function, ultimately ending in the characteristic Chagas cardiomyopathy [47]. Our findings suggest that similar mechanisms might be at play during *T. brucei* infection.

There was no increase in the B cell population in the heart. This is somewhat surprising, since antibodies are the major mediators of immune clearance of *T. brucei*, and B cells are crucial for systemic anti-trypanosomal immunity [40]. However, our findings are consistent with other tissue-specific flow cytometry experiments during *T. brucei* infection, which have identified no changes in number of B cells in the lungs or adipose bodies of *T. brucei*-infected mice [13,48]. In contrast, other models of myocarditis and heart failure show that intracardiac B cell populations are increased and play a major pathologic role during viral myocarditis and myocardial infarction [49–54]. It is possible that B cell activation plays a role in *T. brucei*-associated cardiac disease, even if there is no expansion of local populations.

We found limited evidence of a sex-specific difference in *T. brucei*-associated cardiac disease. Male mice exhibited higher NT-proBNP at 33 dpi, higher numbers of intracardiac immune cells, and more severe echocardiographic changes than females, although these differences were not statistically significant. Our findings are in agreement with evidence that HAT is more severe in men than women and is consistent with data indicating that myocarditis is more common in men than women [55,56]. Further work will be needed to expand on these observations and dissect the mechanistic basis of sex differences in HAT.

Much about *T. brucei*-associated cardiac disease remains unknown, and there are serious gaps in our current knowledge, which this animal model could be used to investigate. Our findings raise concerns about long-term, post-treatment consequences of *T. brucei* infection. Most HAT patients are identified and treated, permanently clearing infection. However, the severity of the myocarditis reported by ourselves and others suggests that heart function could be permanently impaired [18–22,28,38,39]. If so, anti-parasitic treatment would not fully alleviate the cardiac symptoms of HAT, since self-directed inflammation could continue even with the removal of the

313 inciting stimulus. Moreover, this suggests that immunomodulatory therapies could be considered
314 for treatment of both humans and cattle to suppress inflammation that could contribute to
315 persistent heart disease. There is a necessity to investigate the long-term and post-treatment
316 consequences of *T. brucei*-associated myocarditis to determine whether HAT patients are at
317 increased lifetime risk of heart failure [29,46]
318
319 In summary, we describe the first reproducible, optimized, clinically relevant murine model of *T.*
320 brucei-associated cardiac disease, a feature of African trypanosomiasis that is often overlooked
321 in current textbooks and clinical resources [53,54]. In the context of this model's characterization,
322 we produced evidence suggesting that *T. brucei*-associated cardiac damage is an immune-
323 mediated event. Future studies with this model will be instrumental in identifying potential
324 treatments for cardiac manifestations of African trypanosomiasis, a disease which continues to
325 take an extensive human and economic toll in large regions of the world.
326
327
328 **Methods**
329
330 **Mouse and parasite strains and infection**
331 Male and female C57Bl/6J mice (WT, strain# 000664 Jackson Laboratory) between 7-10 weeks
332 old were each infected by intravenous tail vein injection with ~5 pleiomorphic EATRO 1125
333 AnTat1.1E 90-13 *T. brucei* parasites. To quantify parasitemia, blood was collected from the tail
334 vein every two 2 days starting at 4 days post-infection (dpi), and parasites were counted via
335 hemocytometer (Supplemental Figure 1). Blood (125 uL) was collected by a submandibular
336 bleed at terminal endpoint (28 or 33 dpi). Unless otherwise described, mice were euthanized at
337 terminal endpoint by intraperitoneal injection of ketamine/xylazine and perfused with 50 mL of
338 PBS-Glucose (0.055M D-glucose) with heparin to remove intravascular parasites.
339
340 For immunofluorescence experiments, mice were infected intravenously with ~5 AnTat1.1E
341 chimeric triple reporter *T. brucei* parasites which express tdTomato [35]. Parasitemia was measured
342 as previously described. At 14 dpi, mice were sacrificed as previously described.
343
344 For flow cytometry experiments, mice were infected and parasitemia was measured as
345 previously described. Mice were sacrificed at 28 dpi using CO2 euthanasia.
346
347 **Echocardiogram**
348 At 28 dpi, sedated echocardiography was performed on sedated mice by a blinded investigator
349 using a Vevo 2100 Ultrasound System (VisualSonics Inc.) as described previously [58].
350
351 At 33 dpi, echocardiography was performed on awake mice using a 40-MHz transducer
352 (VisualSonics Inc.) as described previously [59].
353
354 **Heart digestion**
355 Heart digestion was performed using a technique previously [60]. Briefly, after sacrifice, mice were
356 perfused with 3 mL Hank's Balanced Salt Solution (HBSS). 60 mg of heart tissue was placed in
357 a 15 mL tube with 3 mL of HBSS. Digestion was performed for half an hour with 300 units of
358 DNase I (Sigma-Aldrich), 625 units of collagenase II (Sigma-Aldrich), and 50 units of

359 hyaluronidase II (Sigma-Aldrich). After digestion, the tubes were centrifuged at 250xg for 5
360 minutes at 4 °C, the supernatant was removed, and the pellet was resuspended in 5 mL ACK
361 lysis buffer (Invitrogen) and incubated for 5 minutes at room temperature to remove red blood
362 cells. Suspended cells were passed through a 50 µm filter and then prepared for flow cytometry.
363
364 **Flow cytometry**
365 Flow cytometry was performed using a technique previously described [60]. Cell suspensions were
366 labeled with fluorescently conjugated antibodies (Supplemental Table 1). FACS was performed
367 on an Aurora Spectral Flow Cytometer (Cytek) and analyses were performed using FlowJo
368 version 10.8.1 (Becton Dickinson).
369
370 **NT-proBNP ELISA**
371 At 28 and 33 dpi, plasma was collected from mice via cheek-bleeding. NT-proBNP plasma
372 levels were measured using the LS-F34395 Mouse NT-proBNP Sandwich ELISA Kit (LSBio)
373 according to the manufacturer's instructions.
374
375 **Histopathology**
376 For histopathology experiments, animals were infected and sacrificed at 28 dpi as previously
377 described. Hearts were placed in 10% neutral buffered formalin and fixed at room temperature
378 for 48 hours. The heart was cut in half longitudinally and sectioned by the Johns Hopkins
379 Oncology Tissue and Imaging Services Core. To evaluate inflammation, hearts were stained with
380 hematoxylin and eosin and imaged with 4x, 10x, and 40x objectives using a Nikon Eclipse E400
381 light microscope (Nikon). Cardiac lesions were graded by a blinded veterinary pathologist using
382 a previously established both the Dallas Criteria and a semiquantitative scoring system for
383 myocarditis in rodents (Table 1) [36,37]. Briefly, the severity and extent of lesions was graded using
384 a five-point system from 0 to 4. A zero score indicates no infiltration. A '1' score indicates very
385 limited focal distribution of myocardial lesions. A '2' score indicates multiple lesions. A '3'
386 score indicates multiple regions with confluence and extensive necrosis. A '4' score indicates
387 lesions affecting most of the observed tissue. Images were captured using an Excelis 4K camera
388 (Unitron) and processed using ImageJ v1.53 image analysis software (NIH). All methods
389 followed published guidelines for experimental pathology [61].
390
391 **Immunofluorescence**
392 For immunofluorescence experiments, 8-week-old female C57Bl/6J mice were infected
393 intravenously with 5 triple marker *T. brucei* parasites [35]. At 14 dpi, mice were euthanized and
394 perfused as previously described. Heart was collected and fixed in 4% paraformaldehyde in PBS
395 for 12 hours at 4 °C. Post-fixation, tissues were sectioned longitudinally, frozen embedded in
396 O.C.T. Compound (Tissue-Tek), and cut using cryostat microtome into 10 µm sections by the
397 Johns Hopkins Oncology Tissue and Imaging Services Core.
398
399 The following antibodies were applied to sections: rat anti-mouse CD-31 (SCBT) followed by
400 goat anti-rat Alexa Fluor 488 (CST). Coverslips were mounted using ProLong Gold (Life
401 technologies). Tissues were imaged with 4x, 10x and 20x objectives using a Nikon Eclipse 90i
402 fluorescence microscope (Nikon) and X-Cite 120 fluorescent lamp (Excelitas) with an ORCA-
403 ER digital CCD camera (Hammamatsu) and ImageJ v1.53 image analysis software (NIH). Image

collection and analysis followed published guidelines for rigor and reproducibility in immunofluorescence [62].

Statistics

Unless otherwise described, figures were generated and statistical analyses were performed using the Tidyverse package in R version 4.2.3[63].

Acknowledgements

We would like to kindly thank Brice Rotureau for providing us with the chimeric triple reporter cell line.

The Aurora Flow Cytometer used in this study was funded by NIH Grant S10OD026859. We acknowledge the support of the JHU Ross Flow Cytometry Core.

Echocardiograms were performed by Nadan Wang of the JHU Small Animal Cardiovascular Phenotyping and Animal Model Core.

Histology support was provided by the JHU Oncology Tissue Services Core, funded by JHU Cancer Center Core Grant P30 CA006973.

This project was supported by the Johns Hopkins Specialized Center for Research Excellence in Sex Differences (U54AG062333) and The Foundation for Gender-Specific Medicine. NPC was supported by T32 OD011089.

450 **Figures**

451

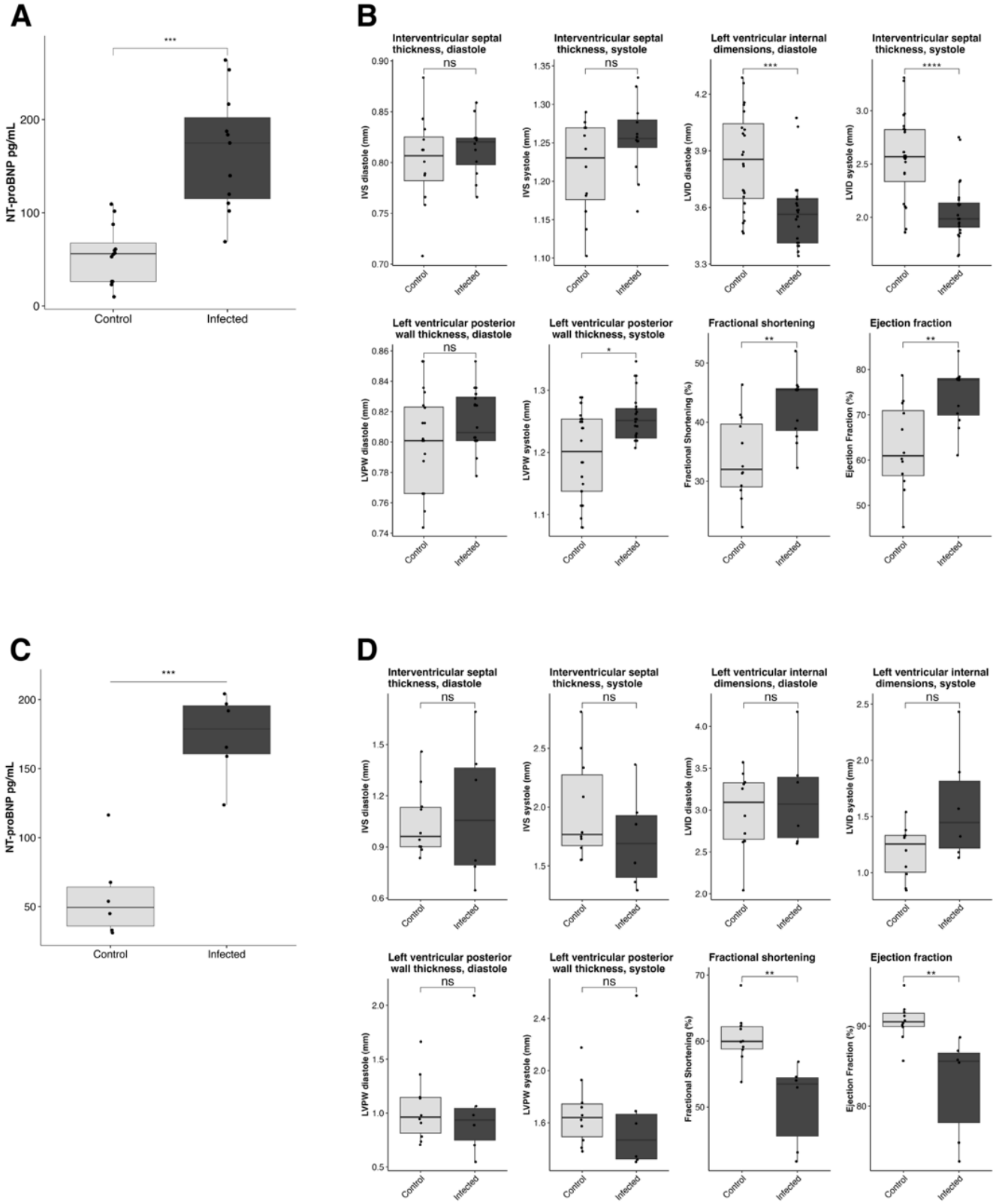

452

453 **Figure 1**. *T. brucei* infection causes elevated NT-proBNP and heart failure with preserved
454 ejection fraction

455 A. Measurement of plasma NT-proBNP at 28 dpi. Plasma NT-proBNP is significantly
456 elevated at 28 dpi (n=12) compared to age-matched uninfected controls (Student's t-test,
457 p=0.00037).
458 B. Echocardiographic measurements at 28 dpi. At 28 dpi, infected mice (n=12) exhibit
459 significantly increased ejection fraction compared to uninfected age-matched controls, as
460 measured by sedated echocardiography (Student's t-test, p=0.0029).
461 C. Measurement of plasma NT-proBNP at 33 dpi. Plasma NT-proBNP is significantly
462 elevated at 33 dpi in infected mice (n=6) compared to uninfected age-matched controls
463 (Student's t-test, p=2.8e-05).
464 D. D. Measurement of ejection fraction at 33 dpi. At 33 dpi, infected mice (n=6) exhibit
465 significantly decreased ejection fraction compared to uninfected age-matched controls,
466 as measured by awake echocardiography (Student's t-test, p=0.011)

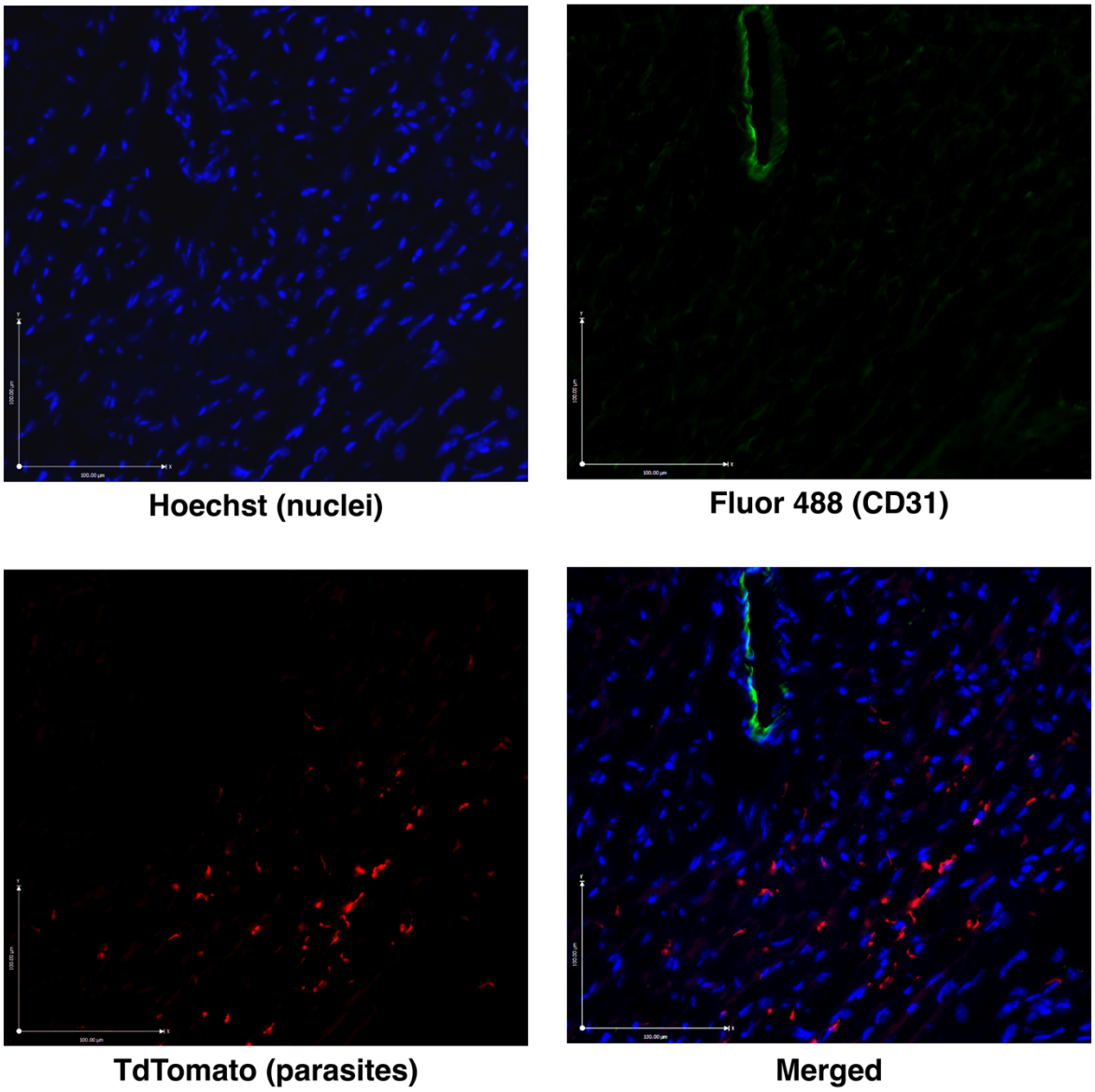

Figure 2. *T. brucei* parasites occupy extravascular spaces in the heart
Representative immunofluorescence microphotographs of the cardiac ventricle at 14 dpi at 20x magnification. *T. brucei* parasites (tdTomato—red) localize separately from CD31-lined vascular structures (Alexa Fluor 488—green), confirming the extravascular localization of parasites. Nuclei are stained with Hoechst (blue).

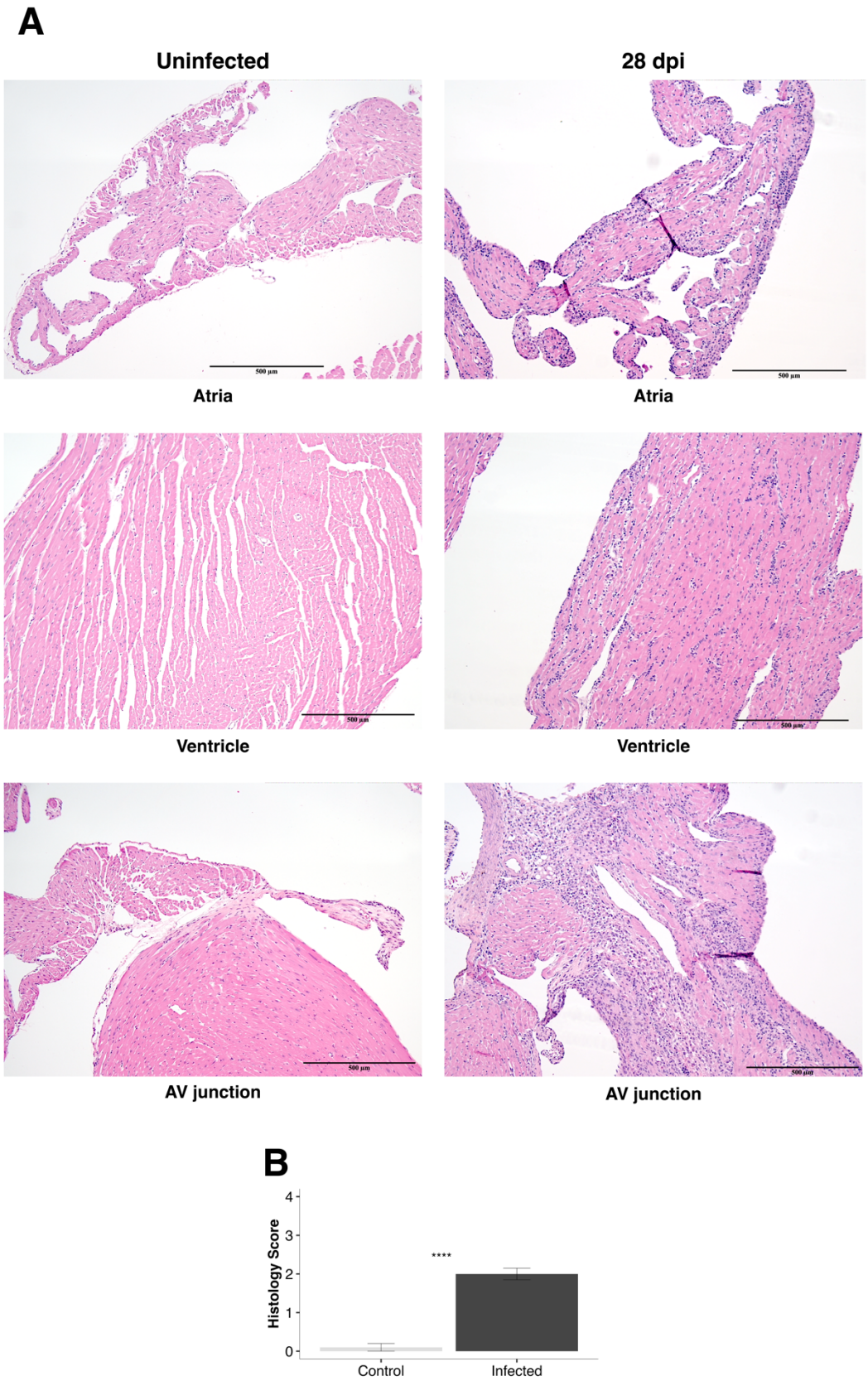
A
Uninfected
28 dpi
Atria
Atria
Ventricle
Ventricle
AV junction
AV junction
B
Histology Score
4
3
2
1
0
****
Control
Infected

476

Figure 3. *T. brucei* infection causes myocarditis at 28 dpi

A. Representative brightfield microphotographs of the heart of infected mice at 28 dpi, compared to uninfected age-matched controls at 10x magnification. Inflammation is present in all layers and regions of the heart and is composed largely of mononuclear cells, primarily lymphocytes, plasma cells, and histiocytes. Inflammation is most severe at the atrioventricular junction.

B. Histological grading of myocarditis (n=6) at 28 dpi, compared to equal numbers of age-matched controls. The average grade at 28 dpi is '2', indicating multifocal moderate myocarditis without extensive associated necrosis. Histological grade is significantly higher in infected than uninfected mice (Student's t test, p=1.5e-8)

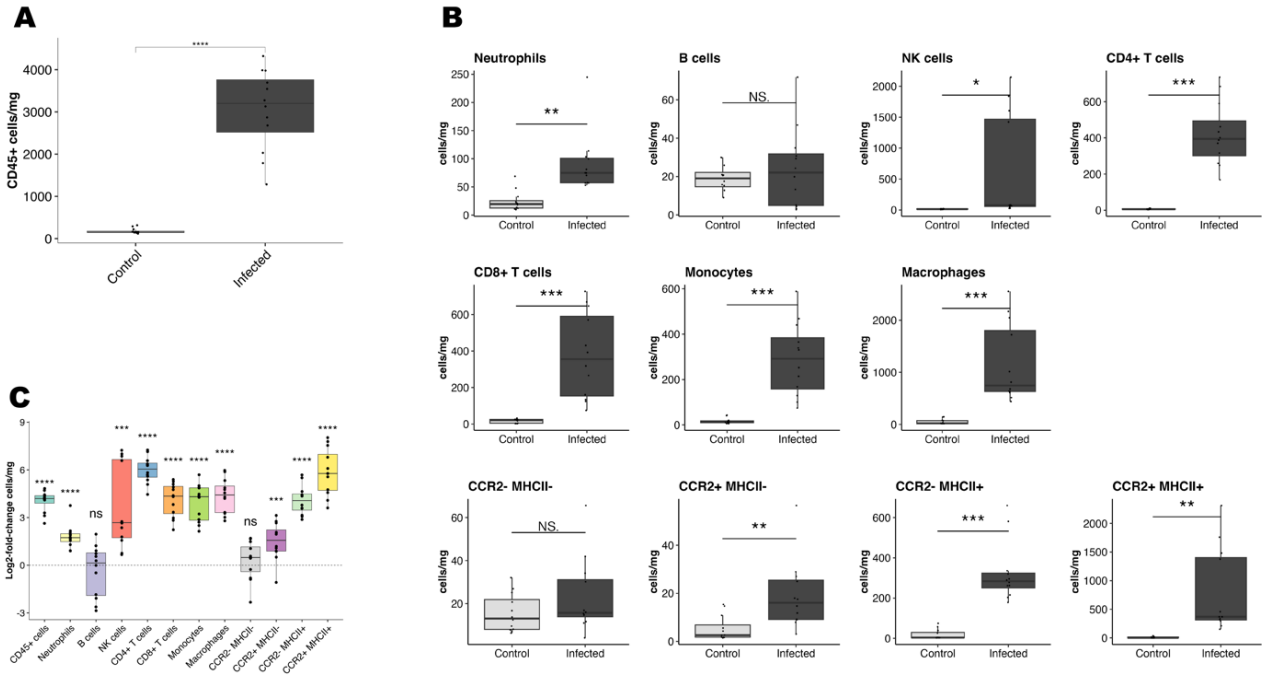

Figure 4. The intracardiac immune cell population during *T. brucei* infection is characteristic of immune-mediated myocarditis

A. Flow cytometric quantification of CD45+ cells per mg. At 28 dpi, CD45+ cells are markedly increased in the hearts of infected mice (n=12) compared to uninfected age-matched controls, supportive of myocarditis (Student's t-test, p= 4.6e-7).

B. Flow cytometric quantification of myeloid and lymphoid cell populations. Most immune cell populations are significantly increased in the hearts of infected mice at 28 dpi. Statistical comparisons were made using Student's t test. *p<0.05, **p<0.01, ***p<0.001.

C. Visualization of magnitude of changes in immune cell populations using the log2-fold change in cells/mg compared to uninfected age-matched control mice calculated based on the average cells/mg in the hearts of uninfected control mice.

Tables

Table 1: Histological grading criteria

Grade	Description
0	No inflammatory infiltrates
1	Limited focal distribution of myocardial lesions
2	Multiple lesions with inflammatory infiltrates and some confluence
3	Multiple lesions with confluence and extensive necrosis
4	Lesions affecting most of the observed tissue

References

1. Holmes, P. Tsetse-transmitted trypanosomes - Their biology, disease impact and control. *Journal of Invertebrate Pathology* vol. 112 Preprint at https://doi.org/10.1016/j.jip.2012.07.014 (2013).
2. Kennedy, P. G. E. & Rodgers, J. Clinical and neuropathogenetic aspects of human African trypanosomiasis. *Frontiers in Immunology* vol. 10 Preprint at https://doi.org/10.3389/fimmu.2019.00039 (2019).
3. Spickler, A. R. African Animal Trypanosomiasis. *IO State University Center for Food Security and Public Health* (2018).
4. Franco, J. R. *et al.* The elimination of human African trypanosomiasis: Achievements in relation to WHO road map targets for 2020. *PLoS Negl Trop Dis* **16**, (2022).
5. Funk, S., Nishiura, H., Heesterbeek, H., Edmunds, W. J. & Checchi, F. Identifying Transmission Cycles at the Human-Animal Interface: The Role of Animal Reservoirs in Maintaining Gambiense Human African Trypanosomiasis. *PLoS Comput Biol* **9**, (2013).
6. Njiokou, F. *et al.* Wild fauna as a probable animal reservoir for Trypanosoma brucei gambiense in Cameroon. *Infection, Genetics and Evolution* **6**, 147–153 (2006).
7. Njiokou, F. *et al.* Domestic animals as potential reservoir hosts of Trypanosoma brucei gambiense in sleeping sickness foci in Cameroon. *Parasite* **17**, 61–6 (2010).
8. Abro, Z. *et al.* The potential economic benefits of controlling trypanosomiasis using waterbuck repellent blend in sub-Saharan Africa. *PLoS One* **16**, (2021).
9. Trindade, S. *et al.* Trypanosoma brucei Parasites Occupy and Functionally Adapt to the Adipose Tissue in Mice. *Cell Host Microbe* **19**, 837–848 (2016).
10. Poltera, A. A. Pathology of human African trypanosomiasis with reference to experimental African trypanosomiasis and infections of the central nervous system. *Br Med Bull* **41**, 169–174 (1985).
11. Crilly, N. P. & Mugnier, M. R. Thinking outside the blood: Perspectives on tissue-resident Trypanosoma brucei. *PLoS Pathogens* vol. 17 Preprint at https://doi.org/10.1371/journal.ppat.1009866 (2021).
12. De Niz, M. *et al.* Organotypic endothelial adhesion molecules are key for Trypanosoma brucei tropism and virulence. *Cell Rep* **36**, (2021).
13. Machado, H. *et al.* Trypanosoma brucei triggers a broad immune response in the adipose tissue. *PLoS Pathog* **17**, (2021).
14. Wolbach, S. B. & Binger, C. A. A Contribution to the Parasitology of Trypanosomiasis. *J Med Res* **27**, 83-108.13 (1912).
15. Blum, J. A. *et al.* Sleeping hearts: The role of the heart in sleeping sickness (human African trypanosomiasis). *Tropical Medicine and International Health* **12**, 1422–1432 (2007).
16. Tsala Mbala, P., Blackett, K., Mbonifor, C. L., Leke, R. & Etoundi, J. [Functional and immunologic involvement in human African trypanosomiasis caused by Trypanosoma gambiense]. *Bull Soc Pathol Exot Filiales* **81**, 490–501 (1988).
17. Hawking, F. & Greenfield, J. G. Two autopsies on rhodesiense sleeping sickness; Visceral lesions and significance of changes in cerebrospinal fluid. *Trans R Soc Trop Med Hyg* **35**, 155–156 (1941).
18. Poltera, A. A., Cox, J. N. & Owor, R. Pancarditis affecting the conducting system and all valves in human African trypanosomiasis. *Heart* **38**, 827–837 (1976).

19. Poltera, A. A., Sayer, P. D., Rudin, W. & Bovell, D. Trypanosomal cardiac valvulitis in vervet monkeys. *Tropical Medicine and Parasitology* **36**, 77–80 (1985).
20. Ikede, B. O. & Losos, G. J. Pathology of the disease in sheep produced experimentally by Trypanosoma brucei. *Vet Pathol* **9**, 278–289 (1972).
21. Ikede, B. O. & Losos, G. J. Pathological changes in cattle infected with Trypanosoma brucei. *Vet Pathol* **9**, 272–277 (1972).
22. Morrison, W. I., Murray, M., Sayer, P. D. & Preston, J. M. The pathogenesis of experimentally induced Trypanosoma brucei infection in the dog I. Tissue and organ damage. *American Journal of Pathology* **102**, 168–181 (1981).
23. McCarroll, C. S., Rossor, C. L., Morrison, L. R., Morrison, L. J. & Loughrey, C. M. A Pre-clinical Animal Model of Trypanosoma brucei Infection Demonstrating Cardiac Dysfunction. *PLoS Negl Trop Dis* **9**, (2015).
24. Elliott, E. B. *et al.* Trypanosoma brucei cathepsin-L increases arrhythmogenic sarcoplasmic reticulum-mediated calcium release in rat cardiomyocytes. *Cardiovasc Res* **100**, 325–335 (2013).
25. Wildner, G. Are rats more human than mice? *Immunobiology* **224**, 172–176 (2019).
26. Kennedy, P. G. E. Animal models of human African trypanosomiasis-very useful or too far removed? *Transactions of the Royal Society of Tropical Medicine and Hygiene* vol. 101 1061–1062 Preprint at https://doi.org/10.1016/j.trstmh.2007.05.001 (2007).
27. Chatelain, E. & Konar, N. Translational challenges of animal models in chagas disease drug development: A review. *Drug Design, Development and Therapy* vol. 9 4807–4823 Preprint at https://doi.org/10.2147/DDDT.S90208 (2015).
28. Poltera, A. A., Hochmann, A. & Lambert, P. H. A model for cardiopathy induced by Trypanosoma brucei brucei in mice. A histologic and immunopathologic study. *American Journal of Pathology* **99**, 325–352 (1980).
29. Galvao-Castro, B., Hochmann, A. & Lambert, P. H. The role of the host immune response in the development of tissue lesions associated with African trypanosomiasis in mice. *Clin Exp Immunol* **33**, 12–24 (1978).
30. Beaver, A. K. *et al.* Extravascular spaces are the primary reservoir of antigenic diversity in Trypanosoma brucei infection. *bioRxiv* 2022.06.27.497797 (2023) doi:10.1101/2022.06.27.497797.
31. Yancy, C. W. *et al.* 2017 ACC/AHA/HFSA Focused Update of the 2013 ACCF/AHA Guideline for the Management of Heart Failure: A Report of the American College of Cardiology/American Heart Association Task Force on Clinical Practice Guidelines and the Heart Failure Society of America. *J Am Coll Cardiol* **70**, 776–803 (2017).
32. Ranek, M. *et al.* Pathophysiology of heart failure and an overview of therapies. in *Cardiovascular Pathology* (eds. Buja, L. & Butany, J.) (Academic Press).
33. Sara, B. *et al.* Are high NT-proBNP levels more related to inflammation than to left ventricular systolic dysfunction in acute myocarditis? *Eur Heart J Acute Cardiovasc Care* **10**, (2021).
34. Moady, G., Perlmutter, S. & Atar, S. The Prognostic Value of Natriuretic Peptides in Stable Patients with Suspected Acute Myocarditis: A Retrospective Study. *J Clin Med* **11**, 2472 (2022).
35. Calvo-Alvarez, E., Cren-Travaillé, C., Crouzols, A. & Rotureau, B. A new chimeric triple reporter fusion protein as a tool for in vitro and in vivo multimodal imaging to monitor the

development of African trypanosomes and Leishmania parasites. *Infection, Genetics and Evolution* **63**, 391–403 (2018).

36. Thomas Aretz, H. Myocarditis: The Dallas criteria. *Hum Pathol* **18**, 619–624 (1987).
37. Aly, M., Wiltshire, S., Chahrour, G., Loredo Osti, J. C. & Vidal, S. M. Complex genetic control of host susceptibility to coxsackievirus B3-induced myocarditis. *Genes Immun* **8**, 193–204 (2007).
38. Dupont, B., Charmot, G. & Lapresle, C. [Trypanosomiasis presenting with trypanids and complicated by myopericarditis (author's transl)]. *Nouv Presse Med* **8**, 1579–81 (1979).
39. Büngener, W. & Mehlitz, D. [Experimental Trypanosoma infections in Cameroon dwarf goats: histopathological observations (author's transl)]. *Tropenmed Parasitol* **27**, 405–10 (1976).
40. Onyilagha, C. & Uzonna, J. E. Host Immune Responses and Immune Evasion Strategies in African Trypanosomiasis. *Frontiers in Immunology* vol. 10 Preprint at https://doi.org/10.3389/fimmu.2019.02738 (2019).
41. Dick, S. A. *et al.* Self-renewing resident cardiac macrophages limit adverse remodeling following myocardial infarction. *Nat Immunol* **20**, 29–39 (2019).
42. Cohen, C. D. *et al.* Myocardial Immune Cells: The Basis of Cardiac Immunology. *The Journal of Immunology* **210**, 1198–1207 (2023).
43. Liu, G. *et al.* Distinct contributions of CD4+ and CD8+ T cells to pathogenesis of trypanosoma brucei infection in the context of gamma interferon and interleukin-10. *Infect Immun* **83**, 2785–2795 (2015).
44. Frenkel, D. *et al.* Trypanosoma brucei Co-opts NK Cells to Kill Splenic B2 B Cells. *PLoS Pathog* **12**, (2016).
45. De Baetselier, P. *et al.* Alternative versus classical macrophage activation during experimental African trypanosomosis. *Int J Parasitol* **31**, 575–587 (2001).
46. Quintana, J. F. *et al.* The murine meninges acquire lymphoid tissue properties and harbour autoreactive B cells during chronic Trypanosoma brucei infection. *bioRxiv* 2023.04.30.538710 (2023) doi:10.1101/2023.04.30.538710.
47. Bonney, K. M. & Engman, D. M. Autoimmune pathogenesis of chagas heart disease: Looking back, looking ahead. *American Journal of Pathology* vol. 185 1537–1547 Preprint at https://doi.org/10.1016/j.ajpath.2014.12.023 (2015).
48. Mabille, D. *et al.* Impact of pulmonary African trypanosomes on the immunology and function of the lung. *Nat Commun* **13**, (2022).
49. Zouggari, Y. *et al.* B lymphocytes trigger monocyte mobilization and impair heart function after acute myocardial infarction. *Nat Med* **19**, 1273–1280 (2013).
50. Tschöpe, C. *et al.* Myocarditis and inflammatory cardiomyopathy: current evidence and future directions. *Nature Reviews Cardiology* vol. 18 169–193 Preprint at https://doi.org/10.1038/s41569-020-00435-x (2021).
51. Tschöpe, C. *et al.* Targeting CD20+ B-lymphocytes in inflammatory dilated cardiomyopathy with rituximab improves clinical course: a case series. *Eur Heart J Case Rep* **3**, (2019).
52. Mo, F. *et al.* Are activated B cells involved in the process of myocardial fibrosis after acute myocardial infarction? An in vivo experiment. *BMC Cardiovasc Disord* **21**, (2021).
53. Bermea, K., Bhalodia, A., Huff, A., Rousseau, S. & Adamo, L. The Role of B Cells in Cardiomyopathy and Heart Failure. *Current Cardiology Reports* vol. 24 935–946 Preprint at https://doi.org/10.1007/s11886-022-01722-4 (2022).

54. Adamo, L. *et al.* Modulation of subsets of cardiac B lymphocytes improves cardiac function after acute injury. *JCI Insight* **3**, (2018).
55. Fairweather, D. L. *et al.* Sex and gender differences in myocarditis and dilated cardiomyopathy: An update. *Frontiers in Cardiovascular Medicine* vol. 10 Preprint at https://doi.org/10.3389/fcvm.2023.1129348 (2023).
56. Pépin, J., Mpia, B. & Iloasebe, M. Trypanosoma brucei gambiense African trypanosomiasis: Differences between men and women in severity of disease and response to treatment. *Trans R Soc Trop Med Hyg* **96**, 421–426 (2002).
57. Hoffman, K. *et al.* Alterations to the Cardiac Metabolome Induced by Chronic T. cruzi Infection Relate to the Degree of Cardiac Pathology. *ACS Infect Dis* **7**, 1638–1649 (2021).
58. Fitch, M. L. *et al.* Cadmium exposure induces a sex-dependent decline in left ventricular cardiac function. *Life Sci* **324**, (2023).
59. Sørensen, L. L. *et al.* Echocardiographic characterization of a murine model of hypertrophic obstructive cardiomyopathy induced by cardiac-specific overexpression of epidermal growth factor receptor 2. *Comp Med* **66**, 268–277 (2016).
60. Bermea, K. C., Rousseau, S. T. & Adamo, L. Flow Cytometry-Based Quantification and Analysis of Myocardial B-cells. *Journal of Visualized Experiments* **2022**, (2022).
61. Scudamore, C. L. *et al.* Recommendations for minimum information for publication of experimental pathology data: MINPEPA guidelines. *Journal of Pathology* vol. 238 359–367 Preprint at https://doi.org/10.1002/path.4642 (2016).
62. Lee, J. Y. & Kitaoka, M. A beginner's guide to rigor and reproducibility in fluorescence imaging experiments. *Molecular Biology of the Cell* vol. 29 1519–1525 Preprint at https://doi.org/10.1091/mbc.E17-05-0276 (2018).
63. Wickham, H. *et al.* Welcome to the Tidyverse. *J Open Source Softw* **4**, 1686 (2019).